

# 艾灸调控 MEK/ERK 信号通路增强曲美替尼对乳腺癌小鼠的抗肿瘤疗效及机制研究

李继娟, 张晨曦, 梁新月, 马 钰, 刘敬萱, 贾春生, 潘丽佳  
(河北中医药大学针灸推拿学院, 石家庄 050200)

**【摘要】** 目的:探讨艾灸联合丝裂原活化蛋白激酶激酶(MEK)/细胞外信号调节激酶(ERK)通路抑制剂曲美替尼对乳腺癌荷瘤小鼠肿瘤生长的协同抑制作用,并分析其潜在机制。方法:将50只BALB/C雌性小鼠随机分为空白组、模型组、抑制剂组(曲美替尼)、直接灸组、联合组(曲美替尼+直接灸),每组10只。以4T1细胞注射建立乳腺癌荷瘤小鼠模型。予空白组与模型组小鼠0.1 mL 0.9%氯化钠溶液灌胃,每日1次;予抑制剂组小鼠曲美替尼溶液灌胃,3 mg/kg,每日1次;予直接灸组小鼠双侧“足三里”直接灸,每穴每次灸2壮,每2日1次;联合组同时给予曲美替尼溶液灌胃和直接灸干预;各组干预21 d。测量记录小鼠干预前后的体质量和干预后肿瘤体积,称取肿瘤质量、计算抑瘤率,HE染色观察肿瘤组织病理形态变化,免疫组织化学染色法和Western blot法检测小鼠肿瘤组织中磷酸化(p)-MEK、p-ERK、细胞Myc原癌基因(c-Myc)、程序性死亡配体1(PD-L1)蛋白表达情况,实时荧光定量PCR法检测小鼠肿瘤组织中c-Myc、PD-L1的mRNA表达情况。结果:干预后,与空白组比较,模型组小鼠体质量下降( $P<0.01$ )。与模型组比较,各治疗组小鼠体质量均升高( $P<0.01$ ),肿瘤组织形态出现不同程度退变与细胞破裂,肿瘤体积与质量均下降( $P<0.01$ ,  $P<0.05$ ),肿瘤组织中p-MEK、p-ERK、c-Myc、PD-L1阳性表达和蛋白表达,c-Myc与PD-L1的mRNA表达水平降低( $P<0.01$ ,  $P<0.05$ )。与抑制剂组比较,直接灸组小鼠体质量升高( $P<0.01$ ),肿瘤组织p-MEK与p-ERK阳性表达和蛋白表达水平上升( $P<0.01$ ,  $P<0.05$ );联合组小鼠体质量升高( $P<0.05$ ),肿瘤体积与质量下降( $P<0.05$ ),肿瘤组织形态退变与细胞破裂更明显,肿瘤组织中c-Myc、PD-L1阳性表达、蛋白表达水平和mRNA表达水平下降( $P<0.01$ ,  $P<0.05$ )。与直接灸组比较,联合组小鼠肿瘤体积与质量下降( $P<0.01$ ),肿瘤组织形态退变与细胞破裂更明显,肿瘤组织中p-MEK、p-ERK、c-Myc、PD-L1阳性表达、蛋白表达和c-Myc、PD-L1 mRNA表达均下降( $P<0.01$ ,  $P<0.05$ )。结论:艾灸可通过抑制MEK/ERK通路磷酸化及下游c-Myc/PD-L1轴,增强曲美替尼的抗肿瘤效果。

**【关键词】** 艾灸;乳腺癌;丝裂原活化蛋白激酶激酶/细胞外信号调节激酶通路;曲美替尼;协同抗肿瘤;程序性死亡配体1

## Moxibustion enhances the antitumor efficacy of Trametinib in breast cancer-bearing mice via MEK/ERK signaling pathway

LI Ji-juan, ZHANG Chen-xi, LIANG Xin-yue, MA Yu, LIU Jing-xuan, JIA Chun-sheng, PAN Li-jia (College of Acupuncture-moxibustion and Tuina, Hebei University of Chinese Medicine, Shijiazhuang 050200, China)

**【ABSTRACT】 Objective** To explore the synergistic inhibitory effect of moxibustion and mitogen-activated protein kinase kinase (MEK)/ extracellular regulated protein kinases (ERK) pathway inhibitor Trametinib on tumor growth in breast cancer tumor-bearing mice and to analyze its underlying mechanisms. **Methods** Fifty female BALB/C mice were randomly divided into blank control, model, inhibitor (Trametinib), direct moxibustion and combination (Trametinib+moxibustion) groups, with 10 mice in each group. Injection of 4T1 cells was used to establish breast cancer tumor-bearing mouse model. Both the blank control and model groups received gavage of 0.1 mL of normal

【DOI】10.13702/j.1000-0607.20251015

引用格式:李继娟,张晨曦,梁新月,等.艾灸调控MEK/ERK信号通路增强曲美替尼对乳腺癌小鼠的抗肿瘤疗效及机制研究[J].针刺研究,2026,51(4):474-483.

项目来源:河北省自然科学基金项目(No.H2023423029);河北中医药大学2022年博士科研基金项目(No.BSZ2022006)

通信作者:潘丽佳, E-mail:panlijia369@126.com

saline once daily. In the inhibitor group, Trametinib solution was administered by gastric gavage at 3 mg/kg, once a day for 21 d. For mice of the direct moxibustion group, moxibustion was applied at bilateral "Zusanli" (ST36), 2 cones per acupoint, once every 2 days for 21 d. The combination group was treated with administration of Trametinib (once daily) by gastric gavage and direct moxibustion (once every 2 d) for 21 d. Body weight and tumor volumes were measured in mice. The tumor weight was quantified and the tumor inhibition rate was calculated. Histopathological alterations in tumor tissues were observed after H.E. staining. The protein expression levels of phosphorylated (p)-MEK, p-ERK, myelocytomatosis viral oncogene homolog (c-Myc), and programmed cell death ligand 1 (PD-L1) in the tumor tissues were assessed using immunohistochemical staining and Western blot, separately. Additionally, the mRNA expression levels of c-Myc and PD-L1 in the tumor tissue were detected using fluorescence quantitative real-time PCR.

**Results** After the intervention, compared with the blank control group, the body mass of mice was decreased evidently in both the model and inhibitor groups ( $P<0.01$ ), rather than in the direct moxibustion and combination groups. Compared with the model group, the body mass of mice was obviously increased ( $P<0.01$ ), and the tumor volume and weight were obviously decreased in each treatment group ( $P<0.01$ ,  $P<0.05$ ). The tumor inhibition rate was 35.19% in the inhibitor group, 30.27% in the direct moxibustion group, and 50.67% in the combination group. The protein expression levels of p-MEK, p-ERK, c-Myc and PD-L1, and the mRNA expression levels of c-Myc and PD-L1 in the tumor tissues were significantly decreased ( $P<0.01$ ) in each treatment group relatively to the model group. The therapeutic effect of the combination group was significantly superior to that of the inhibitor group in increasing the body mass, and to that of the inhibitor and direct moxibustion groups in reducing the tumor volume, tumor weight, and in down-regulating the immunoactivity and protein and mRNA expressions of c-Myc and PD-L1 ( $P<0.05$ ,  $P<0.01$ ). The therapeutic effect of the combination group was also strikingly superior to that of the direct moxibustion group in down-regulating the immunoactivity and expressions of p-MEK and p-ERK ( $P<0.01$ ,  $P<0.05$ ). The effect of the direct moxibustion group was superior to that of the inhibitor group in increasing the body mass and up-regulating the immunoactivity and protein expressions of p-MEK and p-ERK ( $P<0.01$ ,  $P<0.05$ ). H.E. staining showed that the tumor cells in model group were irregularly arranged and shaped, with obvious cell atypia and enlarged nuclei, but those in the 3 treatment groups displayed obvious cribriform tumor cell degeneration, with more cell debris and smaller density. The degeneration of tumor cells in the combination group was the most obvious. **Conclusion** Moxibustion can enhance the anti-tumor effect of Trametinib by inhibiting the phosphorylation of MEK/ERK pathway and the downstream c-Myc/PD-L1 axis in mice with breast cancer, which provides an experimental basis for the adjuvant targeting therapy of breast cancer with moxibustion.

**【KEYWORDS】** Moxibustion; Breast cancer; MEK/ERK pathway; Trametinib; Synergistic anticancer; Programmed cell death ligand 1

乳腺癌是一种具有不同分子亚型的异质性疾病,根据2022年全球癌症统计报告,乳腺癌已成为仅次于肺癌的全球第二大常见恶性肿瘤,在被诊断患有癌症的女性患者中,乳腺癌的死亡人数最高<sup>[1-2]</sup>。当前乳腺癌的临床治疗方法主要是手术切除、化学治疗、放射治疗和免疫治疗等<sup>[3-4]</sup>,但这些治疗方法的总体效果仍不能让人满意,存在术后复发、疗效不确定、免疫耐药等诸多问题<sup>[5]</sup>。近年来,丝裂原活化蛋白激酶激酶(MEK)/细胞外信号调节激酶(ERK)信号通路作为调控肿瘤增殖与免疫逃逸的关键通路,其抑制剂(如曲美替尼)在乳腺癌治疗中展现出一定的潜力,但单药治疗效果有限,且易产生耐药性<sup>[6-9]</sup>。因此,探索能够增强MEK/ERK抑制剂疗效的辅助疗法具有重要意义。

临床已有研究证明艾灸作为辅助疗法能够减

轻乳腺癌患者癌后疲乏,缓解淋巴水肿,减轻放、化疗不良反应,提高机体免疫力<sup>[10-12]</sup>。课题组前期研究结果显示,艾灸能够下调乳腺癌小鼠肿瘤组织中程序性死亡受体1(PD-1)/程序性死亡配体1(PD-L1)等免疫检查点的表达,并抑制肿瘤生长<sup>[13]</sup>。在乳腺癌中,MEK/ERK信号通路的异常激活会诱导细胞Myc原癌基因(c-Myc)表达,而c-Myc会从转录水平上促进PD-L1在肿瘤微环境中的表达,增加免疫逃逸<sup>[14-15]</sup>,而艾灸能否增强MEK/ERK抑制剂的疗效,更好地抑制乳腺癌生长有待验证。因此本研究通过观察艾灸与MEK抑制剂曲美替尼联合干预对MEK/ERK通路关键分子、c-Myc及下游免疫检查点PD-L1的影响,探讨艾灸辅助靶向治疗的效果和作用机制,为优化乳腺癌综合治疗方案提供新思路。

## 1 材料与方法

### 1.1 实验动物与分组

50只6周龄SPF级BALB/C雌性小鼠,体质量为15~20 g,购于北京维通利华生物科技有限公司,生产许可证号:SCXK(京)2021-0006。造模前适应性喂养1周,饲养环境:室温20~25℃,湿度50%~60%,所有小鼠自由摄食饮水,予以普通饲料喂养。1周后随机分为空白组、模型组、抑制剂组、直接灸组、联合组,每组10只。所有动物相关实验操作遵循科技部颁布的《关于善待实验动物的指导性意见》,本研究方案已通过河北中医药大学动物伦理审查委员会批准(审批编号:DWLL202312009)。

### 1.2 主要仪器和试剂

艾绒(河南优诺康),电子天平(福建华志电子科技),游标卡尺(浙江德力西),病理切片机(上海徠卡),离心机(美国赛默飞),实时荧光定量PCR仪(北京鲲鹏基因),光学显微镜(日本Nikon),高速组织研磨仪(武汉赛维尔),发光仪(广州博鹭腾),酶标仪(美国BioTek),垂直电泳仪和转膜仪(美国BIO-RAD)。

曲美替尼(美国MCE),培养基(美国Gibco),动物组织RNA提取试剂盒(美国OMEGA),HE染液(武汉赛维尔),ECL超敏化学发光试剂盒(美国GLP BIO),免疫组织化学DAB显色剂(北京索莱宝),cDNA合成试剂盒(北京金沙),qPCR SYBR荧光染料(北京金沙),PCR引物(上海生工),4T1细胞(广州辉俊),c-Myc、磷酸化(p)-MEK1/2抗体(美国Affinity),ERK1/2、p-ERK1/2、PD-L1、MEK1/2、GAPDH抗体(美国Proteintech)。

### 1.3 模型制备

小鼠适应性饲养1周后脱毛。取出冻存的小鼠乳腺癌4T1细胞复苏、培养、传代。细胞消化离心,加入细胞培养基质胶,调整细胞浓度为 $1 \times 10^6$ 个/mL,异氟烷麻醉小鼠后,取0.1 mL混有肿瘤细胞的基质胶注射于小鼠左侧第四乳头脂肪垫下。造模后观察7 d,以接种处出现皮下肿瘤,高凸隆起坚硬,肿瘤体积增大至 $4.5 \text{ mm} \times 4.5 \text{ mm} \times 4.5 \text{ mm}$ ,为造模成功<sup>[16]</sup>。

### 1.4 干预措施

小鼠造模成功后进行干预,穴位定位参照《实验动物常用穴位名称与定位 第3部分:小鼠》<sup>[17]</sup>,选取双侧“足三里”作为施灸部位。各组小鼠采取相同时间的抓取与固定。空白组与模型组小鼠给予

0.1 mL 0.9%氯化钠溶液灌胃,每日1次。抑制剂组灌胃0.1 mL曲美替尼溶液(3 mg/kg),每日1次<sup>[18]</sup>。直接灸组小鼠在双侧“足三里”皮肤处涂抹凡士林,称取0.5 mg的艾绒,自制成直径约1 mm,形似麦粒的艾炷,用镊子夹取艾炷平稳置于“足三里”处,点燃艾炷,每穴每次2壮,每2 d 1次。联合组同时给予曲美替尼灌胃和直接灸干预。各组干预均持续21 d。干预期间每2 d测量记录1次小鼠体质量及肿瘤大小,观察小鼠生存状态,若小鼠肿瘤体积超过 $12.5 \text{ mm} \times 12.5 \text{ mm} \times 12.5 \text{ mm}$ 则提前终止实验。

### 1.5 观察指标及检测方法

测量每组小鼠体质量与肿瘤体积:干预前后测量小鼠体质量;干预结束后用游标卡尺测量肿瘤瘤体的长(L, mm)和宽(W, mm),计算公式为肿瘤体积( $\text{mm}^3$ )= $(L \times W^2) \times 0.5$ 。

取材:实验结束以后,称取记录小鼠取材前最终体质量,异氟烷麻醉小鼠后脱颈处死,在冰盒上迅速剥离小鼠肿瘤,称重并记录。随后将小鼠肿瘤组织分为两部分,一部分4%多聚甲醛固定48 h用于制作石蜡切片,另一部分迅速投入液氮中保存,随后转移至-80℃冰箱用于后续检测。

小鼠抑瘤率测定:迅速剥离肿瘤后称重,计算公式为抑瘤率( $\%$ )= $(\text{模型组平均肿瘤质量} - \text{各组平均肿瘤质量}) \div \text{模型组平均肿瘤质量} \times 100\%$

HE染色法评估小鼠肿瘤组织病理学变化:取固定于多聚甲醛中的肿瘤组织制作石蜡切片。每组随机选择6只小鼠的石蜡切片(厚 $4 \mu\text{m}$ ),将切片烘干脱蜡复水,苏木精染色后冲洗,组织分化液分化冲洗,伊红溶液染色,脱水透明,透明封片胶封片。使用200倍光学显微镜观察肿瘤组织病理学变化。

免疫组织化学法检测小鼠肿瘤组织中p-MEK、p-ERK、c-Myc、PD-L1的阳性表达:每组随机选取8只小鼠的石蜡切片,烤片,脱蜡修复,内源性过氧化物酶阻断剂孵育,封闭后滴加p-MEK(1:50)、p-ERK(1:100)、c-Myc(1:50)、PD-L1(1:500)一抗 $4^\circ\text{C}$ 过夜。第2天切片恢复室温,滴反应增强液孵育,再滴加二抗孵育。用配制的DAB显色液显色,纯水终止显色,滴加苏木精,脱水透明,透明封片胶封片。每张切片于光学显微镜下随机选取4个视野观测,阳性着色为棕褐色,采用Image J图像分析软件分析读取阳性表达区域覆盖率,区域覆盖率( $\%$ )= $\text{阳性区域面积} \div \text{参考区域总面积} \times 100\%$ 。

Western blot法检测小鼠肿瘤组织中MEK、

p-MEK、ERK、p-ERK、c-Myc、PD-L1 蛋白表达: 每组随机选择8只小鼠的肿瘤组织, 称取肿瘤组织后裂解, 研磨离心, BCA法测定总蛋白浓度。加蛋白上样缓冲液, 加热、冷却后上样, 电泳, 转膜, 奶粉封闭, 加入 MEK(1:30 000)、p-MEK(1:3 000)、ERK(1:10 000)、p-ERK(1:5 000)、c-Myc(1:1 000)、PD-L1(1:800)、GAPDH(1:70 000)一抗孵育过夜; 加入二抗(1:8 000)室温孵育, 洗涤, 滴加 ECL 发光液, 凝胶成像系统自动成像。用 Image J 软件分析条带灰度值, 以目的蛋白条带与内参 GAPDH 条带灰度值比值作为目的蛋白的相对表达量, 并计算 p-MEK/MEK, p-ERK/ERK 比值。

实时荧光定量 PCR 法检测小鼠肿瘤组织中 c-Myc、PD-L1 的 mRNA 表达: 取每组 8 只小鼠的肿瘤组织 30 mg, 使用 RNA 提取试剂盒提取肿瘤组织总 RNA。检测 RNA 浓度和纯度后, 反转录合成 cDNA 并进行扩增。反应体系: 上下游引物各 0.4  $\mu$ L, cDNA 2  $\mu$ L, 2 $\times$ GS AntiQ qPCR SYBR Fast Mix(Universal) 10  $\mu$ L, 加入双蒸水至 20  $\mu$ L。反应条件: 95  $^{\circ}$ C 预变性 30 s; 95  $^{\circ}$ C 变性 10 s, 60  $^{\circ}$ C 退火 10 s, 72  $^{\circ}$ C 延伸 30 s, 循环 40 次。以 GAPDH 为内参, 采用  $2^{-\Delta\Delta C_t}$  法计算目的基因的相对表达量。引物序列见表 1。

表 1 引物序列  
Table 1 Primer sequences

基因	序列(5'→3')	产物长度/bp
c-Myc	上游 TCGCTGCTGTCTCCGAGTCC	150
	下游 GGTGTTGCTCTTCTCCACAGAC	
PD-L1	上游 GCTCCAAAGGACTTGTACGTG	238
	下游 TGATCTGAAGGGCAGCATTTTC	
GAPDH	上游 AGGTCGGTGTGAACGGATTTG	123
	下游 TGTAGACCATGTAGTTGAGGTCA	

注: c-Myc 为细胞 Myc 原癌基因, PD-L1 为程序性死亡配体 1。

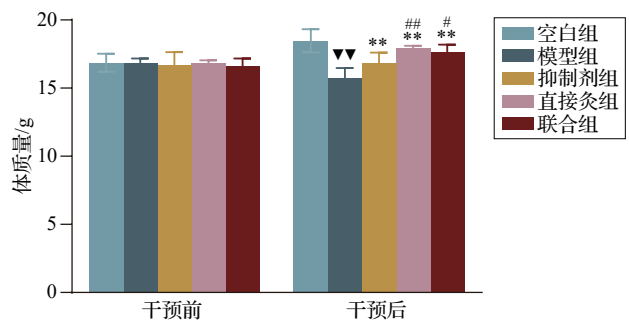
### 1.6 统计学分析

采用 SPSS26.0 统计软件进行分析处理, GraphPad Prism 9.0 软件绘制图片。所有数据均为计量资料, 符合正态分布, 以均数 $\pm$ 标准差( $\bar{x}\pm s$ )表示, 组间比较采用单因素方差分析, 方差齐时组间两两比较用 LSD 法, 方差不齐时采用 Tamhane's  $t_2$  法。以  $P\leq 0.05$  为差异有统计学意义的标准。

## 2 结果

### 2.1 各组小鼠干预前后体质量比较

干预前, 各组小鼠体质量差异无统计学意义。干预后, 与空白组比较, 模型组小鼠体质量下降 ( $P<0.01$ ); 与模型组比较, 各治疗组小鼠体质量均升高 ( $P<0.01$ ); 与抑制剂组比较, 直接灸组与联合组小鼠体质量升高 ( $P<0.01, P<0.05$ )。其余各组两两比较差异无统计学意义, 见图 1。



注: 与空白组比较,  $\blacktriangledown P<0.01$ ; 与模型组比较,  $**P<0.01$ ; 与抑制剂组比较,  $\#P<0.05, \#\#P<0.01$ 。

图 1 各组小鼠干预前后体质量比较 ( $\bar{x}\pm s$ , 10 只鼠/组)

Fig. 1 Comparison of body weight of mice in the 5 groups before and after interventions ( $\bar{x}\pm s$ , 10 mice/group)

### 2.2 各组小鼠肿瘤体积比较

取材后各组小鼠肿瘤如图 2 所示。干预结束后, 与模型组比较, 各治疗组小鼠肿瘤体积均下降 ( $P<0.01, P<0.05$ ); 与抑制剂组、直接灸组比较, 联合组小鼠肿瘤体积下降 ( $P<0.05, P<0.01$ )。其余各组两两比较差异无统计学意义, 见图 3。

### 2.3 各组小鼠肿瘤质量及抑瘤率比较

与模型组比较, 各治疗组小鼠肿瘤质量均明显下降 ( $P<0.01$ ); 与抑制剂组、直接灸组比较, 联合组小鼠肿瘤质量下降 ( $P<0.05, P<0.01$ )。其余各组两两比较差异无统计学意义, 见图 4。抑制剂组小鼠抑瘤率为 35.19%, 直接灸组小鼠抑瘤率为 30.27%, 联合组小鼠抑瘤率为 50.67%, 见表 2。

### 2.4 各组小鼠肿瘤组织病理形态比较

HE 染色结果显示, 各组小鼠的肿瘤细胞排列不规整, 形态不规则, 细胞异形明显, 细胞核增大。抑制剂组、直接灸组和联合组小鼠的肿瘤组织出现明显的筛网状细胞退变, 并多见细胞碎片, 密度变小, 其中联合组肿瘤细胞退变最为明显, 见图 5。

### 2.5 各组小鼠肿瘤组织中 p-MEK、p-ERK、c-Myc、PD-L1 阳性表达比较

与模型组比较, 各治疗组小鼠肿瘤组织中

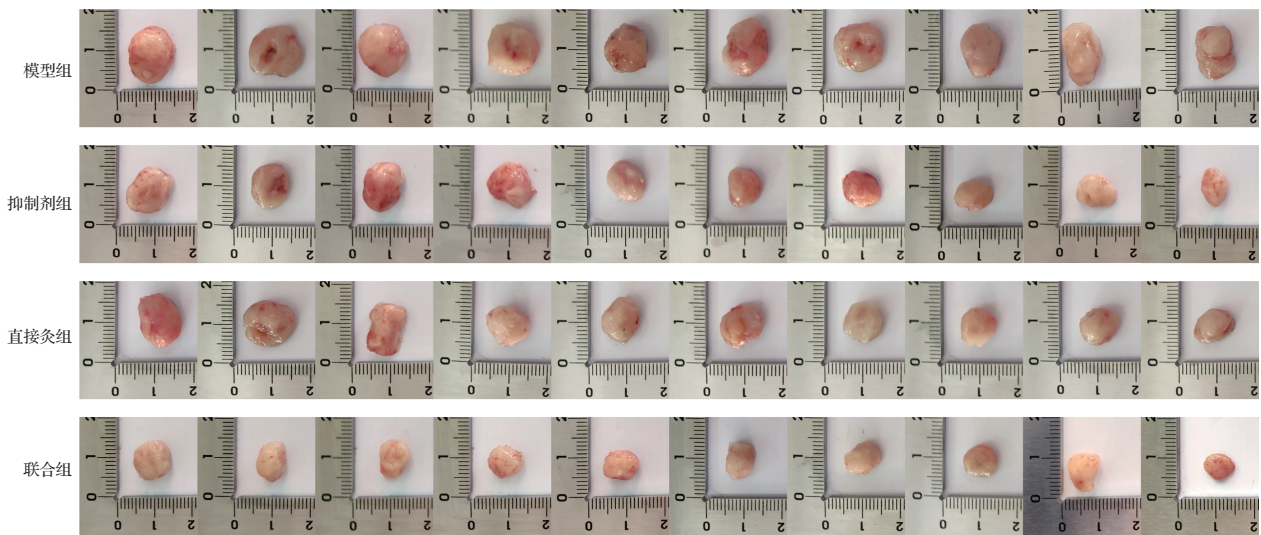
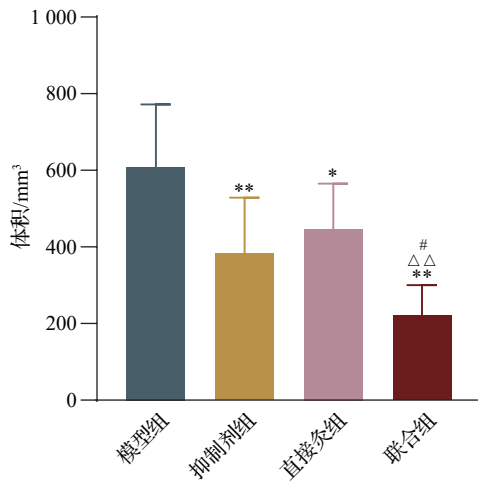


图2 各组小鼠肿瘤实体图(最小刻度为1 mm)

Fig. 2 Tumors images of mice in the 4 groups (minimum scale division: 1 mm)



注:与模型组比较,\* $P<0.05$ ,\*\* $P<0.01$ ;与抑制剂组比较,  
# $P<0.05$ ;与直接灸组比较,△△ $P<0.01$ 。

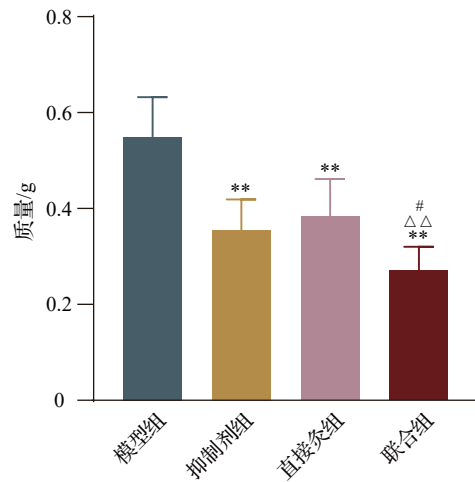
图3 各组乳腺癌荷瘤小鼠干预后肿瘤体积比较  
( $\bar{x}\pm s$ , 10只鼠/组)

Fig. 3 Comparison of the tumor volume of breast cancer-bearing mice in the 4 groups after interventions  
( $\bar{x}\pm s$ , 10 mice/group)

p-MEK、p-ERK、c-Myc、PD-L1 阳性表达均下降 ( $P<0.01$ );与抑制剂组比较,直接灸组肿瘤组织中 p-MEK、p-ERK 阳性表达升高 ( $P<0.01$ ),联合组肿瘤组织中 c-Myc、PD-L1 阳性表达下降 ( $P<0.01$ );与直接灸组小鼠相比,联合组肿瘤组织中 p-MEK、p-ERK、c-Myc、PD-L1 阳性表达下降 ( $P<0.01$ )。其余各组两两比较差异无统计学意义,见图6。

### 2.6 各组小鼠肿瘤组织中 p-MEK、p-ERK、c-Myc、PD-L1 蛋白表达比较

与模型组比较,各干预组小鼠肿瘤组织中



注:与模型组比较,\*\* $P<0.01$ ;与抑制剂组比较,# $P<0.05$ ;  
与直接灸组比较,△△ $P<0.01$ 。

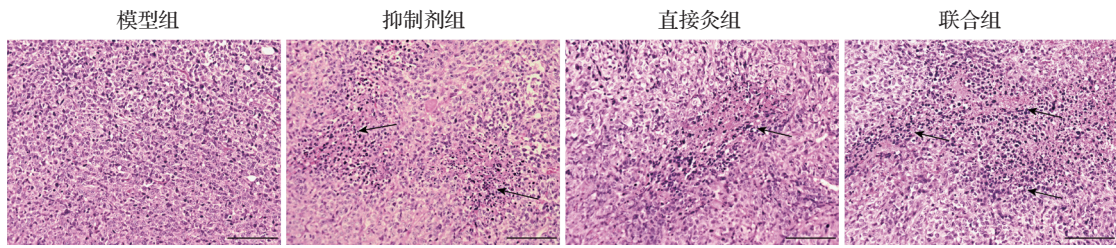
图4 各组乳腺癌荷瘤小鼠肿瘤质量比较( $\bar{x}\pm s$ , 10只鼠/组)  
Fig. 4 Comparison of tumor weight of breast cancer-bearing mice in the 4 groups ( $\bar{x}\pm s$ , 10 mice/group)

表2 各组小鼠抑瘤率比较

Table 2 Comparison of tumor inhibition rate of mice in the 4 groups

组别	动物数/只	抑瘤率/%
模型组	10	-
抑制剂组	10	35.19
直接灸组	10	30.27
联合组	10	50.67

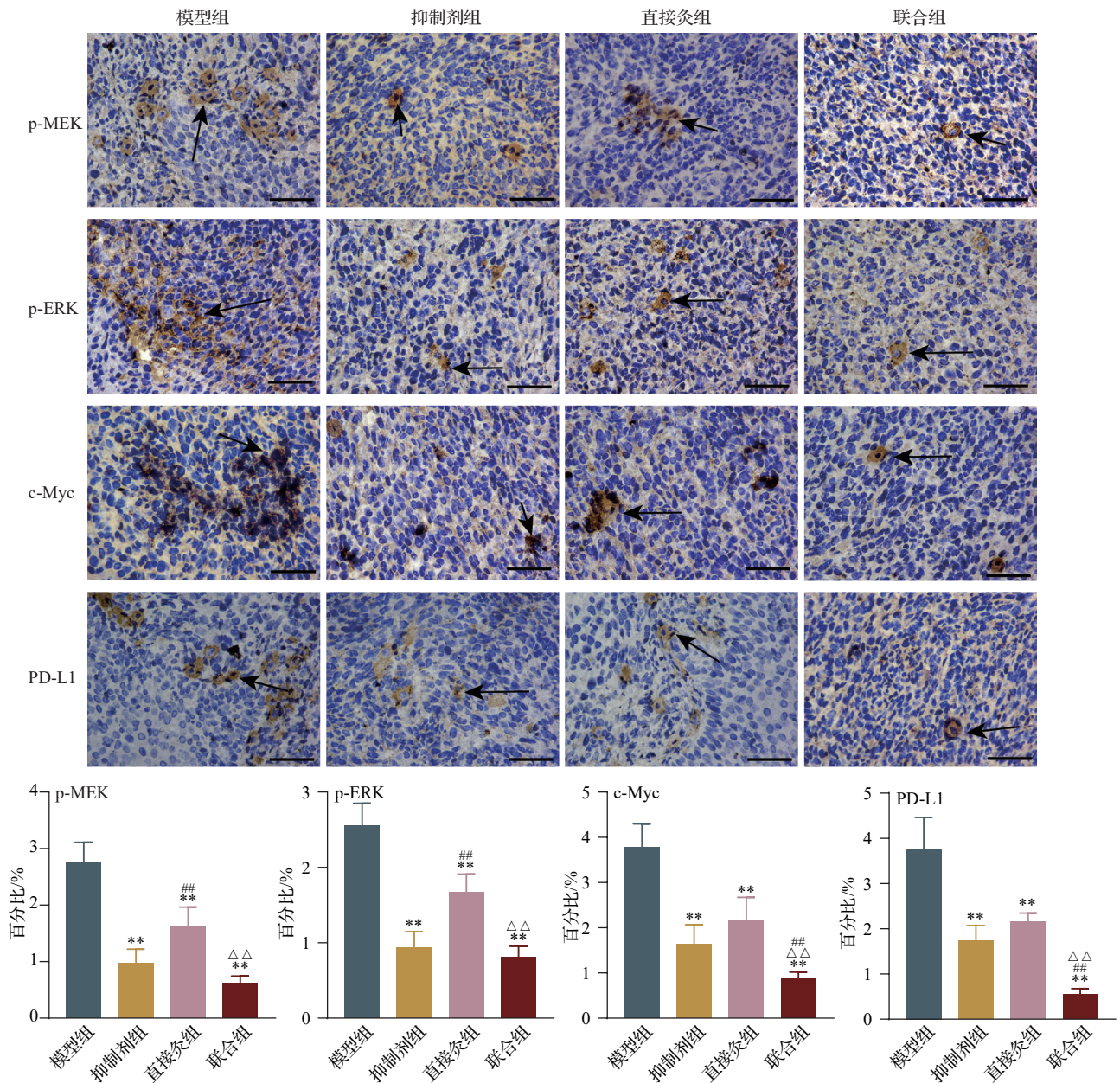
p-MEK、p-ERK、c-Myc、PD-L1 蛋白表达均下降 ( $P<0.01$ ,  $P<0.05$ );与抑制剂组比较,直接灸组肿瘤组织中 p-MEK、p-ERK 蛋白表达升高 ( $P<0.05$ ),



注:标尺=100 μm,黑色箭头示肿瘤细胞破裂碎片及退变。

图5 各组乳腺癌荷瘤小鼠肿瘤组织病理形态比较(HE染色)

Fig. 5 Comparison of pathological morphology of tumor tissue of breast cancer-bearing mice in the 4 groups (HE staining)



注:p-MEK为磷酸化丝裂原活化蛋白激酶, p-ERK为磷酸化细胞外调节蛋白激酶, c-Myc为细胞Myc原癌基因, PD-L1为程序性死亡配体1。标尺=50 μm,图中黑色箭头所示为阳性表达区域。与模型组比较,\*\* $P < 0.01$ ;与抑制剂组比较,## $P < 0.01$ ;与直接灸组比较, $\Delta\Delta P < 0.01$ 。

图6 各组乳腺癌荷瘤小鼠肿瘤组织中p-MEK、p-ERK、c-Myc、PD-L1阳性表达比较(免疫组织化学染色,  $\bar{x} \pm s$ , 8只鼠/组)

Fig. 6 Comparison of the positive expression of p-MEK, p-ERK, c-Myc and PD-L1 in tumor tissue of breast cancer-bearing mice in the 4 groups (immunohistochemical staining,  $\bar{x} \pm s$ , 8 mice/group)

联合组肿瘤组织中 c-Myc、PD-L1 蛋白表达下降 ( $P<0.05$ );与直接灸组小鼠比较,联合组肿瘤组织中 p-MEK、p-ERK、c-Myc、PD-L1 蛋白表达下降 ( $P<0.05, P<0.01$ )。其余各组两两比较差异无统计学意义,见图 7。

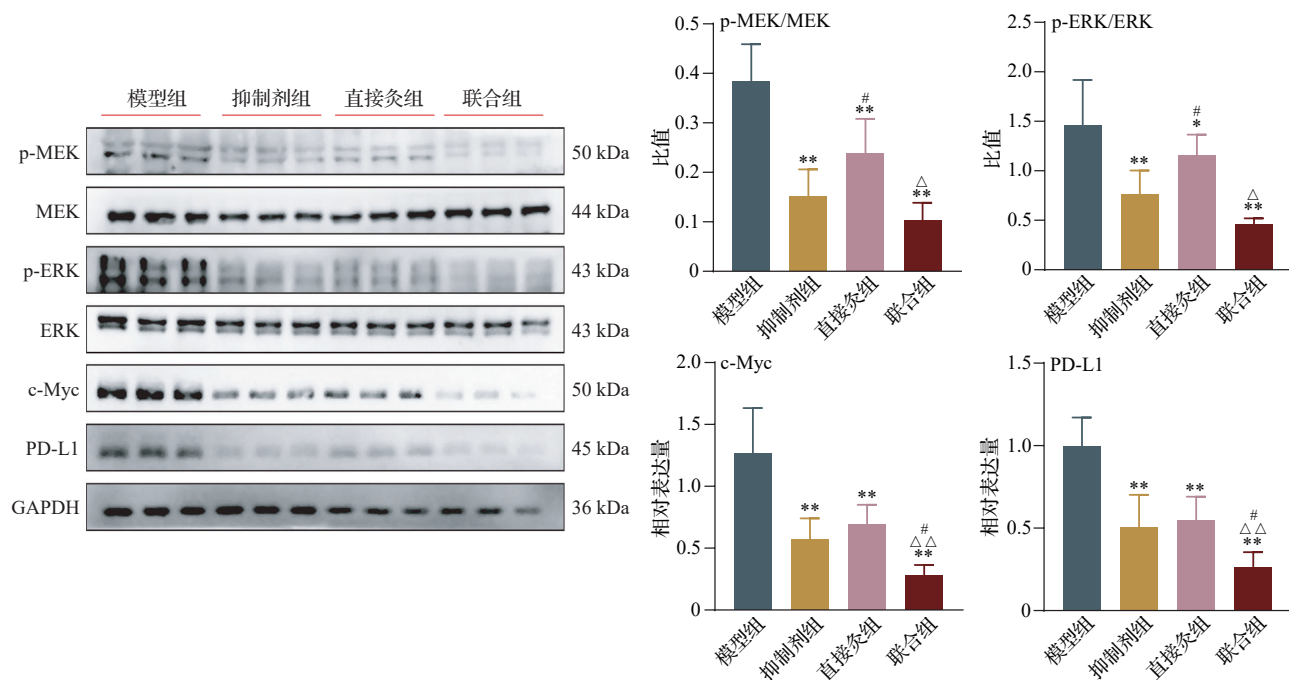
### 2.7 各组小鼠肿瘤组织中 c-Myc、PD-L1 的 mRNA 表达比较

与模型组比较,各治疗组小鼠肿瘤组织中

c-Myc、PD-L1 的 mRNA 表达下降 ( $P<0.01$ );与抑制剂组、直接灸组比较,联合组小鼠肿瘤组织中 c-Myc、PD-L1 的 mRNA 表达下降 ( $P<0.01$ )。其余各组两两比较差异无统计学意义,见图 8。

### 3 讨论

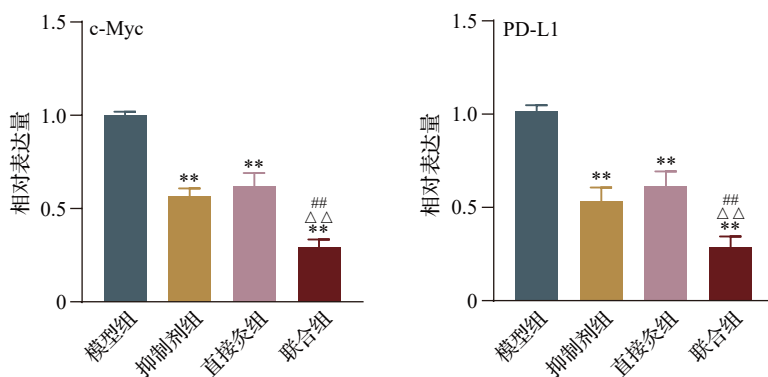
乳腺癌又称为“石痈”“乳岩”“石奶”“乳石”“翻花石榴发”“翻花奶”等,被归于痈疽类疾病范畴<sup>[19]</sup>。



注:p-MEK为磷酸化丝裂原活化蛋白激酶激酶,MEK为丝裂原活化蛋白激酶激酶,p-ERK为磷酸化细胞外调节蛋白激酶,ERK为细胞外调节蛋白激酶,c-Myc为细胞Myc原癌基因,PD-L1为程序性死亡配体1。与模型组比较,\* $P<0.05$ ,\*\* $P<0.01$ ;与抑制剂组比较,# $P<0.05$ ;与直接灸组比较,△ $P<0.05$ ,△△ $P<0.01$ 。

图 7 各组乳腺癌荷瘤小鼠肿瘤组织中 p-MEK、p-ERK、c-Myc、PD-L1 蛋白表达比较 ( $\bar{x}\pm s$ , 8 只鼠/组)

Fig. 7 Comparison of the protein expression levels of p-MEK, p-ERK, c-Myc and PD-L1 in tumor tissue of breast cancer-bearing mice in the 4 groups ( $\bar{x}\pm s$ , 8 mice/group)



注:c-Myc为细胞Myc原癌基因,PD-L1为程序性死亡配体1。与模型组比较,\*\* $P<0.01$ ;与抑制剂组比较,## $P<0.01$ ;与直接灸组比较,△△ $P<0.01$ 。

图 8 各组乳腺癌荷瘤小鼠肿瘤组织中 c-Myc、PD-L1 的 mRNA 表达水平比较 ( $\bar{x}\pm s$ , 8 只鼠/组)

Fig. 8 Comparison of the mRNA expression levels of c-Myc and PD-L1 in tumor tissue of breast cancer-bearing mice in the 4 groups ( $\bar{x}\pm s$ , 8 mice/group)

《外科正宗》中提到“忧郁伤肝,思虑伤脾,积想在心,所愿不得志者,致经络痞涩,聚结成核”,阐述了乳腺癌的病因病机,本虚标实是乳腺癌发病的根本<sup>[20]</sup>。艾灸是通过作用于皮肤表面的温热刺激,结合经络腧穴及艾叶的功效治疗疾病,能够温经通络、散瘀消结、固本培元、调和阴阳<sup>[21]</sup>。足三里作为胃经合穴,胃腑之下合穴,与机体免疫系统密切相关,具有补益气血、增强正气、扶正祛邪的作用<sup>[22]</sup>。艾灸“足三里”能够抑制结直肠癌细胞肝转移<sup>[23]</sup>;艾灸“足三里”可缓解肺癌荷瘤小鼠化疗后的骨髓抑制<sup>[24]</sup>。目前尚未有研究报道临床单独直接灸抑制肿瘤生长,临床中主要用于辅助治疗,改善肿瘤的相关临床症状,如艾灸足三里辅助治疗能够改善乳腺癌患者免疫状态,下调肿瘤标志物水平<sup>[25]</sup>。但有动物实验研究证实麦粒灸能够减缓肺癌小鼠瘤体生长,抑制炎症信号分子<sup>[26]</sup>;麦粒灸“足三里”能够有效抑制肝癌荷瘤小鼠肿瘤生长,增加荷瘤小鼠体质量<sup>[27]</sup>。在本实验中,抑制剂、直接灸及联合组的小鼠体质量均相比模型组上升,且直接灸组上升最为明显,表明艾灸有益于肿瘤小鼠治疗过程中的体质量增加,并且优于抑制剂药物治疗。各治疗组小鼠肿瘤体积与模型组相比较均明显缩小,肿瘤质量下降,肿瘤细胞破裂退变明显,说明曲美替尼、直接灸、曲美替尼与直接灸联合治疗都能够有效抑制乳腺癌肿瘤生长,并且联合组小鼠表现出最小的肿瘤体积和最高抑瘤率,这提示艾灸增强了曲美替尼的干预效果和其对肿瘤生长的抑制作用。

MEK/ERK 信号通路是促进肿瘤增殖和抑制凋亡的经典信号通路<sup>[28]</sup>,在包括乳腺癌在内的多种癌症中被证明可以促进肿瘤的生长转移<sup>[29-31]</sup>。已有研究结果显示,MEK/ERK 信号通路的激活促进了乳腺癌的恶性进展<sup>[32-33]</sup>。c-Myc 是 Myc 基因家族中的关键成员之一,参与细胞代谢、增殖和分化,作为 ERK 信号通路的下游效应分子,它在正常细胞的致癌转化和肿瘤增殖中起着至关重要的作用,被认为是肿瘤生长和免疫逃逸的重要协调者<sup>[34-36]</sup>。有研究结果显示,在肿瘤内皮细胞中抑制 ERK-c-Myc 轴是抑制肿瘤生长的有效策略<sup>[37]</sup>。艾灸“足三里”能够降低大鼠 MEK/ERK 通路中 MEK、ERK 信号分子的磷酸化水平<sup>[38-39]</sup>。热敏灸治疗能有效降低慢性萎缩性胃炎大鼠 c-Myc 表达<sup>[40]</sup>。本研究中,曲美替尼作为 MEK 抑制剂能够抑制 MEK/ERK 通路中的 MEK 与 ERK 磷酸化表达,直接灸也能有效抑制 MEK/ERK 信号通路中 MEK、ERK 磷酸化激活,实

现抗肿瘤作用。3 个治疗组中,联合组小鼠肿瘤组织中 MEK/ERK 信号通路激活水平得到有效抑制,c-Myc 蛋白表达水平下降最为明显,表明联合干预通过 MEK/ERK 通路下调 c-Myc 表达更有优势。

癌细胞采取免疫逃逸的机制之一是表面抑制性配体的表达,如 PD-L1<sup>[41]</sup>。PD-L1 是 PD-1 的配体之一,主要表达于肿瘤细胞和肿瘤微环境中的细胞<sup>[42]</sup>。PD-L1 能与 T 细胞表面的 PD-1 结合,并传递适应性免疫应答的逃逸信号,从而抑制 T 细胞介导的细胞毒性<sup>[43]</sup>。而 c-Myc 能充当转录激活因子,在转录水平结合到 PD-L1 基因的启动子区域,直接诱导 PD-L1 转录的增加<sup>[44]</sup>。已有研究证实,艾灸可以影响 PD-1/PD-L1 相关分子表达,抑制 T 细胞增殖<sup>[45]</sup>。艾灸和隔药饼灸“足三里”干预可明显降低免疫抑制兔外周血中 PD-L1 的表达<sup>[46]</sup>。本实验结果显示,与模型组相比,各治疗组的 PD-L1 蛋白、mRNA 和阳性表达均下调,联合组中的 PD-L1 蛋白、mRNA 和阳性表达下调更为明显,提示联合干预能更好地降低 PD-L1 表达,抑制肿瘤生长。

总之,本实验提示,艾灸可通过抑制 MEK/ERK 通路磷酸化及下游 c-Myc/PD-L1 轴,显著增强曲美替尼对 MEK/ERK 通路的抑制效应,并协同降低 PD-L1 表达,更有效地抑制乳腺癌小鼠的肿瘤生长,增强曲美替尼的抗肿瘤效果,为艾灸辅助靶向治疗乳腺癌提供了实验依据。此次实验尚未选择通路相关激动剂全面评估,未来也将进一步验证并探索艾灸辅助治疗肿瘤的其他优势与相关作用机制。

**利益冲突** 所有作者声明不存在利益冲突。作者贾春生为本刊编委,但未参与本文的审理。

## 参考文献

- [1] MACKENZIE M, STOBART H, DODWELL D, et al. Risk of breast cancer death after a diagnosis of early invasive breast cancer[J]. *BMJ*, 2023, 381: 1355.
- [2] MICHAELS E, WORTHINGTON R O, RUSIECKI J. Breast cancer: risk assessment, screening, and primary prevention[J]. *Med Clin North Am*, 2023, 107(2): 271-284.
- [3] TURGEON G A, WEICKHARDT A, AZAD A A, et al. Radiotherapy and immunotherapy: a synergistic effect in cancer care[J]. *Med J Aust*, 2019, 210(1): 47-53.
- [4] LOIBL S, POORTMANS P, MORROW M, et al. Breast cancer[J]. *Lancet*, 2021, 397(10286): 1750-1769.
- [5] YU Y X, WANG S, LIU Z N, et al. Traditional Chinese medicine in the era of immune checkpoint inhibitor: theory, development, and future directions[J]. *Chin Med*, 2023, 18(1): 59.

- [6] GUO Y J, PAN W W, LIU S B, et al. ERK/MAPK signalling pathway and tumorigenesis [J]. *Exp Ther Med*, 2020, 19(3): 1997-2007.
- [7] SOMORJAI I M L, EHEBAUER M T, ESCRIVÀ H, et al. JNK mediates differentiation, cell polarity and apoptosis during amphioxus development by regulating actin cytoskeleton dynamics and ERK signalling [J]. *Front Cell Dev Biol*, 2021, 9: 749806.
- [8] HAN H W, YANG M K, WEN Z L, et al. Trametinib and M17, a novel small molecule inhibitor of AKT, display a synergistic antitumor effect in triple negative breast cancer cells through the AKT/mTOR and MEK/ERK pathways [J]. *Bioorg Chem*, 2025, 154: 107981.
- [9] HOEFLICH K P, O' BRIEN C, BOYD Z, et al. In vivo antitumor activity of MEK and phosphatidylinositol 3-kinase inhibitors in basal-like breast cancer models [J]. *Clin Cancer Res*, 2009, 15(14): 4649-4664.
- [10] MAO H J, JIN M, XIE L L, et al. Infrared laser moxibustion for cancer-related fatigue in breast cancer survivors: a randomized controlled trial [J]. *Breast Cancer Res*, 2024, 26(1): 80.
- [11] WANG C H, YANG M, FAN Y Y, et al. Moxibustion as a therapy for breast cancer-related lymphedema in female adults: a preliminary randomized controlled trial [J]. *Integr Cancer Ther*, 2019, 18: 1534735419866919.
- [12] 余婷, 柳华伟, 刘祖琴, 等. 热敏灸辅助姑息治疗提高老年恶性肿瘤患者生存质量: 随机对照试验 [J]. *中国针灸*, 2025, 45(2): 167-172.
- YU T, LIU H W, LIU Z Q, et al. Heat-sensitive moxibustion assisted in palliative treatment to improve the quality of life in elderly patients with malignant tumor: a randomized controlled trial (in Chinese) [J]. *Chinese Acupuncture & Moxibustion*, 2025, 45(2): 167-172.
- [13] 张飞程, 高田宇, 张晨曦, 等. 灸药联合对乳腺癌荷瘤小鼠肿瘤组织免疫检查点的影响 [J]. *针刺研究*, 2025, 50(3): 319-326.
- ZHANG F C, GAO T Y, ZHANG C X, et al. Effect of moxibustion combined with chemotherapy on immune checkpoints in tumor tissue of breast cancer-bearing mice (in Chinese) [J]. *Acupuncture Research*, 2025, 50(3): 319-326.
- [14] YE X X, LIN J M, CHEN Y P, et al. IGF<sub>2</sub>BP<sub>1</sub> accelerates the aerobic glycolysis to boost its immune escape in hepatocellular carcinoma microenvironment [J]. *Front Immunol*, 2024, 15: 1480834.
- [15] XING J, GINTY D D, GREENBERG M E. Coupling of the RAS-MAPK pathway to gene activation by RSK2 a growth factor-regulated CREB kinase [J]. *Science*, 1996, 273(5277): 959-963.
- [16] ZHANG G L, ZHANG Y, CAO K X, et al. Orthotopic injection of breast cancer cells into the mice mammary fat pad [J]. *J Vis Exp*, 2019(143): 143.
- [17] 中国针灸学会. 实验动物常用穴位名称与定位 第3部分: 小鼠 [J]. *针刺研究*, 2021, 46(4): 351-352.
- China Association of Acupuncture and Moxibustion. Nomenclature and location of commonly used acupoints in experimental animals. Part 3: mice (in Chinese) [J]. *Acupuncture Research*, 2021, 46(4): 351-352.
- [18] CHO H, MATSUMOTO S, FUJITA Y, et al. Trametinib plus 4-methylumbelliferone exhibits antitumor effects by ERK blockade and CD44 downregulation and affects PD-1 and PD-L1 in malignant pleural mesothelioma [J]. *J Thorac Oncol*, 2017, 12(3): 477-490.
- [19] 李君, 张丽君, 何慧玲, 等. 古代艾灸治疗乳房肿瘤文献初探 [J]. *中医文献杂志*, 2017, 35(6): 19-21.
- LI J, ZHANG L J, HE H L, et al. An initial research on ancient literature of moxibustion treatment to breast tumors (in Chinese) [J]. *Journal of Traditional Chinese Medical Literature*, 2017, 35(6): 19-21.
- [20] 刘淑珍. 陈实功《外科正宗》灸法简述 [J]. *新疆中医药*, 2024, 42(4): 32-36.
- LIU S Z. Brief introduction of moxibustion in Chen Shigong's *Authentic Surgery* (in Chinese) [J]. *Xinjiang Journal of Traditional Chinese Medicine*, 2024, 42(4): 32-36.
- [21] 洪金标, 彭宏, 易受乡. 艾灸对机体产生的多重效应及其机理探讨 [J]. *中华中医药学刊*, 2010, 28(2): 277-281.
- HONG J B, PENG H, YI S X. Effect of moxibustion on the multiple effects produced by the body and mechanism (in Chinese) [J]. *Chinese Archives of Traditional Chinese Medicine*, 2010, 28(2): 277-281.
- [22] 施茵, 吴焕淦. 足三里穴在免疫功能调节中的应用 [J]. *现代中医药*, 2003, 23(3): 3-6.
- SHI Y, WU H G. Application of Zusanli point in immune function regulation (in Chinese) [J]. *Modern Journal of Traditional Chinese Medicine and Pharmacy*, 2003, 23(3): 3-6.
- [23] 宋亚芳, 张晓梅, 蒋诗媛, 等. 从肠道菌群探讨艾灸“足三里”“肝俞”穴抑制裸鼠结肠癌细胞肝转移机制 [J]. *世界科学技术-中医药现代化*, 2024, 26(12): 3118-3126.
- SONG Y F, ZHANG X M, JIANG S Y, et al. Exploring the mechanism of moxibustion at “Zusanli” and “Ganshu” acupoints in inhibiting liver metastasis of colorectal cancer cells in nude mice from the perspective of gut microbiota (in Chinese) [J]. *Modernization of Traditional Chinese Medicine and Materia Medica-World Science and Technology*, 2024, 26(12): 3118-3126.
- [24] 叶强, 高彤, 梁花花, 等. 艾灸足三里对化疗后骨髓抑制小鼠 Notch 信号通路的影响 [J]. *中国中医基础医学杂志*, 2020, 26(12): 1803-1807.
- YE Q, GAO T, LIANG H H, et al. Effect of moxibustion at Zusanli on Notch signaling pathway in mice with myelosuppression after chemotherapy (in Chinese) [J]. *Journal of Basic Chinese Medicine*, 2020, 26(12): 1803-1807.
- [25] 汪旻琦, 洪月光, 赵莉娜, 等. 慈菇平岩方联合雷火灸对 Luminal 型乳腺癌内分泌治疗敏感性较低患者生殖激素、外周淋巴细胞及 NR3C2、CYFRA21-1 的影响 [J]. *辽宁中医药大学学报*, 2025, 27(8): 177-181.
- WANG M Q, HONG Y G, ZHAO L N, et al. Effects of Cigu pingyan decoction (慈菇平岩方) combined with thunder fire moxibustion on reproductive hormones, peripheral lymphocytes, NR3C2, CYFRA21-1 in patients with luminal breast cancer with low sensitivity to endocrine therapy (in

- Chinese) [J]. Journal of Liaoning University of Traditional Chinese Medicine, 2025, 27(8): 177-181.
- [26] 张雪, 万茜, 徐天舒. 麦粒灸对 Lewis 肺癌小鼠炎症微环境中白介素-6 及信号转导蛋白和转录激活因子 3 的影响[J]. 针刺研究, 2017, 42(3): 235-239.  
ZHANG X, WAN Q, XU T S. Effect of grain-moxibustion on IL-6 and STAT3 in inflammatory microenvironment of lewis lung cancer mice (in Chinese) [J]. Acupuncture Research, 2017, 42(3): 235-239.
- [27] 程艳婷, 朱涛, 马艳竹, 等. 麦粒灸通过调控凋亡因子半胱氨酸家族增强环磷酸胺对 Hepa1-6 肝癌荷瘤小鼠的抗肿瘤作用[J]. 针刺研究, 2023, 48(9): 914-922.  
CHENG Y T, ZHU T, MA Y Z, et al. Moxibustion with seed-size moxa cone enhances anti-tumor effect of cyclophosphamide on Hepa1-6 hepatoma-bearing mice by regulating apoptosis factor cysteine family (in Chinese) [J]. Acupuncture Research, 2023, 48(9): 914-922.
- [28] HE B, GUO L, HU Y W, et al. Desmocollin-2 inhibits cell proliferation and promotes apoptosis in hepatocellular carcinoma via the ERK/c-MYC signaling pathway [J]. Aging (Albany NY), 2022, 14(21): 8805-8817.
- [29] WANG K X, JI W X, YU Y F, et al. Correction: FGFR1-ERK1/2-SOX2 axis promotes cell proliferation, epithelial-mesenchymal transition, and metastasis in FGFR1-amplified lung cancer [J]. Oncogene, 2020, 39(42): 6619-6620.
- [30] YAN Z L, OHUCHIDA K, FEI S, et al. Inhibition of ERK1/2 in cancer-associated pancreatic stellate cells suppresses cancer-stromal interaction and metastasis [J]. J Exp Clin Cancer Res, 2019, 38(1): 221.
- [31] ZHOU X H, LI T, CHEN Y F, et al. Mesenchymal stem cell-derived extracellular vesicles promote the in vitro proliferation and migration of breast cancer cells through the activation of the ERK pathway [J]. Int J Oncol, 2019, 54(5): 1843-1852.
- [32] DO H T T, CHO J. Involvement of the ERK/HIF-1 $\alpha$ /EMT pathway in XCL1-induced migration of MDA-MB-231 and SK-BR-3 breast cancer cells [J]. Int J Mol Sci, 2020, 22(1): 89.
- [33] KUMAR D, PATEL S A, HASSAN M K, et al. Reduced IQGAP2 expression promotes EMT and inhibits apoptosis by modulating the MEK-ERK and p38 signaling in breast cancer irrespective of ER status [J]. Cell Death Dis, 2021, 12(4): 389.
- [34] ZHU P, LI Y, LI P, et al. C-Myc induced the regulation of long non-coding RNA RHPN1-AS1 on breast cancer cell proliferation via inhibiting P53 [J]. Mol Genet Genomics, 2019, 294(5): 1219-1229.
- [35] ZHAO B X, QIAO H X, ZHAO Y, et al. HBV precore G1896A mutation promotes growth of hepatocellular carcinoma cells by activating ERK/MAPK pathway [J]. Virol Sin, 2023, 38(5): 680-689.
- [36] DHANASEKARAN R, DEUTZMANN A, MAHAUAD-FERNANDEZ W D, et al. The MYC oncogene - the grand orchestrator of cancer growth and immune evasion [J]. Nat Rev Clin Oncol, 2022, 19(1): 23-36.
- [37] ZUO Z H, LIU J, SUN Z H, et al. ERK and c-Myc signaling in host-derived tumor endothelial cells is essential for solid tumor growth [J]. Proc Natl Acad Sci USA, 2023, 120(1): e2211927120.
- [38] BI D Y, LIU Q, YI Z, et al. Effect of herbal cake-partitioned moxibustion on MEK1/2 and ERK1/2 expressions of gastric tissues in rats with spleen deficiency syndrome [J]. Journal of Acupuncture and Tuina Science, 2017, 15(5): 305-310.
- [39] 刘琼, 杨宗保, 王晨光, 等. 艾灸“梁门”“足三里”穴对应激性胃溃疡大鼠胃黏膜细胞相关蛋白质磷酸化水平的影响 [J]. 中医杂志, 2014, 55(24): 2129-2133.  
LIU Q, YANG Z B, WANG C G, et al. Influence of moxibustion at acupoints Liangmen (ST21) and Zusanli (ST36) on protein phosphorylation in gastric mucosal cells in rat model of stress gastric ulcers (in Chinese) [J]. Journal of Traditional Chinese Medicine, 2014, 55(24): 2129-2133.
- [40] 章海凤, 罗淑瑜, 张瑶, 等. 热敏灸对慢性萎缩性胃炎模型大鼠 c-myc、survivin、Cyclin D1 的影响 [J]. 时珍国医国药, 2020, 31(3): 746-749.  
ZHANG H F, LUO S Y, ZHANG Y, et al. Effect of heat-sensitive moxibustion on c-myc, survivin and Cyclin D1 in chronic atrophic gastritis model rats (in Chinese) [J]. Lishizhen Medicine and Materia Medica Research, 2020, 31(3): 746-749.
- [41] DONG H D, STROME S E, SALOMAO D R, et al. Tumor-associated B7-H1 promotes T-cell apoptosis: a potential mechanism of immune evasion [J]. Nat Med, 2002, 8(8): 793-800.
- [42] LUO Q Q, SHEN F, ZHAO S, et al. LINC00460/miR-186-3p/MYC feedback loop facilitates colorectal cancer immune escape by enhancing CD47 and PD-L1 expressions [J]. J Exp Clin Cancer Res, 2024, 43(1): 225.
- [43] IWAI Y, HAMANISHI J, CHAMOTO K, et al. Cancer immunotherapies targeting the PD-1 signaling pathway [J]. J Biomed Sci, 2017, 24(1): 26.
- [44] ZHU L L, LIU J W, WANG L, et al. Molecular regulatory network of PD-1/PD-L1 in non-small cell lung cancer [J]. Pathol Res Pract, 2020, 216(4): 152852.
- [45] ZHONG Y M, LAI D L, ZHANG L L, et al. The effects of moxibustion on PD-1/PD-L1-related molecular expression and inflammatory cytokine levels in RA rats [J]. Evid Based Complement Alternat Med, 2021, 2021: 6658946.
- [46] 田岳凤, 李雷勇, 毛凯荣, 等. 不同灸法对免疫抑制兔外周血 PD-1、PD-L1 及免疫细胞分子 CD19、CD45R、CD69、NKG2D 的影响 [J]. 中华中医药学刊, 2021, 39(12): 10-12.  
TIAN Y F, LI L Y, MAO K R, et al. Effects of different moxibustion methods on PD-1 and immune cell molecules CD69, CD19, CD45R and NKG2D in immunosuppressed rabbits (in Chinese) [J]. Chinese Archives of Traditional Chinese Medicine, 2021, 39(12): 10-12.